Deep-Sea Research II ∎ (∎∎∎∎) ∎∎∎–∎∎∎

Contents lists available at ScienceDirect

Deep-Sea Research II

journal homepage: www.elsevier.com/locate/dsr2

Carbonate chemistry in the Northern South China Sea Shelf-sea in June 2010

Xianghui Guo [a,b,*], George T.F. Wong [a]

[a] Research Center for Environmental Changes, Academia Sinica, Taipei 11529, Taiwan
[b] State Key Laboratory of Marine Environmental Science, Xiamen University, Xiamen 361005, Mainland China

ARTICLE INFO

Keywords:
Northern South China Sea Shelf-sea (NoSoCS)
Carbonate chemistry
Aragonite saturation state
Net community production (NCP)
Marginal sea

ABSTRACT

The distributions of dissolved inorganic carbon (C_T), total alkalinity (A_T) and pH at 25 °C (pH_{25}) were determined in the Northern South China Sea Shelf-sea (NoSoCS) in early June, 2010 during a low flow period. The distributions of the partial pressure of CO_2 (pCO_2), *in situ* pH, and temperature normalized pCO_2 ($NpCO_2$) were derived from the measured values. The distribution of A_T is linearly related to salinity indicating that its distribution is controlled primarily by mixing between the surface water and the subsurface North Pacific Tropical Water. Aside from physical mixing, the distribution of C_T is also influenced by its loss through biological uptake and CO_2 evasion to the atmosphere. The net community production (NCP) rate in the NoSoCS is estimated to be 10 ± 20 (with a range of 4–13) mmol C m^{-2} d^{-1}. Within the NoSoCS, the NCP is elevated in the coastal upwelling area, where it is estimated to reach 30 ± 17 mmol C m^{-2} d^{-1}. In addition to temperature, upwelling and biological uptake also affect the distribution of the surface pCO_2 and *in situ* pH.

The waters in the NoSoCS are super-saturated with respect to aragonite at all depths as the saturation horizon is at 600–800 m in the open northern South China Sea. Nevertheless, the aragonite saturation state, Ω_{Ar}, in the surface water, which is mostly between 3.3 and 3.5, is already within the range that has been suggested as barely adequate to marginal for the growth of the tropical shallow-water corals. The Ω_{Ar} is linearly related to *in situ* pH. At the reported rate of pH decrease in the oceans as a result of ocean acidification, Ω_{Ar} might reach a value that is considered "extremely marginal" within several decades and the existence of this type of coral reef ecosystem in the NoSoCS may then be threatened.

1. Introduction

Coastal and marginal seas play an important role in the global carbon cycle since they link the terrestrial, oceanic and atmospheric carbon reservoirs. Although they constitute only ~7% of the ocean by surface area, they contribute 14–30% of the oceanic primary production and 80% of the organic matter burial (Gattuso et al., 1998b). Marginal seas beyond the estuaries are also important sinks of the atmospheric CO_2, contributing 27–30% of the oceanic CO_2 sequestration (Chen and Borges, 2009).

In view of the importance of the marginal seas in oceanic CO_2 sequestration, their carbonate system has been actively studied (Chen and Borges, 2009; Laruelle et al., 2010). However, while the marginal seas at the middle and high latitudes, such as the Middle Atlantic Bight, South Atlantic Bight, the East China Sea, the North Sea, and the Bering Sea have been studied rather extensively (Bates et al., 2011; Cai et al., 2010; Chen and Wang, 1999; Thomas et al., 2004; Wang et al., 2013; Wong, 1979, 1988; Zhai and Dai, 2009), their counterparts in the lower latitudes are still relatively under-studied (Cai et al., 2006; Chen and Borges, 2009; Laruelle et al., 2010). Nevertheless, it is well known that the major processes controlling the carbonate system in the oceans vary with latitude and there is no reason to believe that the marginal seas should be the exception (Cai et al., 2006; Gruber et al., 2009; Takahashi et al., 2009). For example, Cai et al. (2008) report that the global input of bicarbonate to the coastal seas varies with latitude. Wang et al. (2013) find that total alkalinity, A_T, in shelf waters decreases northward along the eastern seaboard of the United States. The recent recognition of ocean acidification (OA) as an imminent global environmental issue (Orr et al., 2005) has provided further impetus for understanding the behavior of the carbonate system in the tropical marginal seas as they may be more susceptible to OA than the open ocean when accompanied by other biogeochemical processes (Cai et al., 2011). Tropical shallow water coral reef ecosystems, which are frequently found in tropical marginal seas, have been predicted as early victims of OA (Gattuso et al., 1998a; Kleypas et al., 1999a; Langdon et al., 2003; Leclercq et al., 2000; Tribollet et al., 2006). Nevertheless, how

* Corresponding author at: State Key Laboratory of Marine Environmental Science, Xiamen University, Xiamen 361005, Mainland China. Tel.: +86 592 2182811.
E-mail address: xhguo@xmu.edu.cn (X. Guo).

http://dx.doi.org/10.1016/j.dsr2.2015.02.024
0967-0645/

the carbonate system in the low latitude marginal seas may respond to terrestrial input, biological processes, local forcing (such as river runoff, coastal upwelling, and atmospheric pumping by tropical cyclones) and exchange with the open ocean are still inadequately documented and understood.

The Northern South China Sea Shelf-sea (NoSoCS) of the northern South China Sea (SCS) is a major sub-tropical coastal sea of the world where coral reef ecosystems are widely found. Previous studies on its carbonate chemistry tend to cover only selected sub-regions and significant sub-regional variations have been found (Zhai et al., 2005, 2009; Dai et al., 2008b; Cao et al., 2011). A characterization of the carbonate system in the NoSoCS as a whole has yet to be attempted. In this study, we report the distributions of dissolved inorganic carbon (C_T), total alkalinity (A_T), pH, pCO_2 and the aragonite saturation state (Ω_{Ar}) in the entire NoSoCS during the early summer of 2010 as an example of the characteristics of the carbonate system in a major sub-tropical marginal sea. Furthermore, the processes controlling these distributions and the response of the NoSoCS to OA are assessed.

2. Material and methods

2.1. Study area

The SCS is located in the northwestern Pacific and extends from 23°N in the sub-tropics at southern Taiwan to 3°S in the tropics at the coasts of Borneo and Sumatra. The NoSoCS is situated at the northwestern corner of the SCS in its subtropical section (Fig. 1). It extends in a northeast to southwest direction from the southern Chinese coast to the shelf edge between 19 and 23°N and between Hainan Island and the southern end of the Taiwan Strait from 110 to 118°E (Fig. 1). The western half of the shelf is narrower and broadens eastward off Shanwei towards Shantou. In response to the southwest monsoon and topographic forcing, a well-documented summer upwelling occurs along the coast in this broadened section of the shelf (Gan et al., 2009a). Vertical mixing within the NoSoCS is also enhanced by internal waves whose occurrence has been observed along the entire outer shelf (Li et al., 2008). The NoSoCS is also the receiving water of a nutrient-rich river draining a heavily urbanized part of the world (Dai et al., 2008a), the Pearl River, whose annual freshwater discharge is about 3.26×10^{11} m^3 (Zhao, 1990). The highest discharge from the Pearl River occurs during the summer and its lowest discharge is in late winter and early spring (Fig. 2). Recently, Liu et al. (2012) report that significant quantities of submarine groundwater may also enter the NoSoCS. While the adjoining open northern SCS is generally oligotrophic (Chen et al., 2001; Chen, 2005; Chen and Chen, 2006; Wong et al., 2007), the biological productivity in the NoSoCS is significantly higher as a result of enhanced vertical mixing and exogenous sources of nutrients (Tan and Shi, 2009).

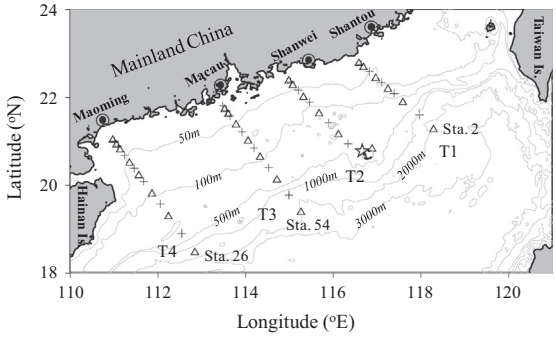

Fig. 1. The study area in the northern South China Sea. Δ – stations along the four transects T1–T4 at which discrete water samples were collected; + – CTD only stations; and open star – Dongsha Atoll.

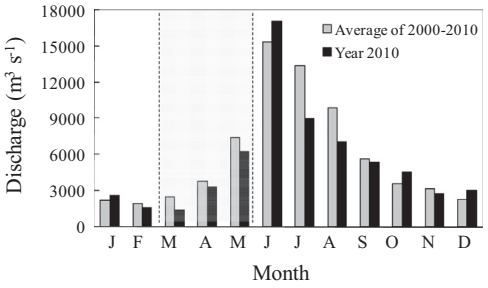

Fig. 2. Monthly averaged freshwater discharge of the largest tributary of the Pearl River system, the West River, at the Wuzhou gauging station (at 111.3290°E, 23.4688°N, Guangxi Zhuang Autonomous Region) (the *Hydrological Information Annual Report* (2000–2010), Ministry of Water Resources, PR China). Shaded area – spring months.

The hydrography and general pattern of circulation in the northern SCS and the NoSoCS are reasonably well known (Chao et al., 1996; Gan et al., 2009a, 2009b; Shaw and Chao, 1994; Wong et al., 2007; Xue et al., 2004). The monsoonal wind is a major forcing of the circulation in the NoSoCS and leads to a generally southwestward flow in the winter and a northeastward flow in the summer (Gan et al., 2006; Xue et al., 2004). However, the details, such as the rate of mass exchange between the NoSoCS and the northern SCS, remain poorly quantified. More extensive reviews on the general oceanography of the NoSoCS appear elsewhere in this special issue (Wong et al., this issue-a, this issue-b).

Previous sub-regional studies on the carbonate chemistry of the NoSoCS were conducted primarily in the summer. Zhai et al. (2005, 2009) report that some sub-regions are sources of CO_2 to the atmosphere, probably as a result of low productivity and high temperature in warm seasons. On the other hand, others (Cao et al., 2011; Dai et al., 2008b) find consistently high uptake rates of dissolved inorganic carbon in the Pearl River plume and in the upwelling waters off the coast between Shantou and Shanwei, where biological productivity is high. A characterization of the carbonate system in the NoSoCS as a whole has yet to be attempted and this information is especially helpful if the impact of OA on the extensive tropical water coral reef ecosystems in the NoSoCS (Guo et al., 1994) is to be assessed.

2.2. Sampling and analysis

Stations were occupied in four cross-shelf transects extending from the inner shelf to the open northern SCS off Shantou, Shanwei, Macou and Maoming from the southern end of the Taiwan Strait (transect T1) to Hainan Island (transect T4), on board R/V Ocean Researcher I (ORI) during cruise ORI 929 on 3–12 June, 2010. At each station, depth profiles of salinity and temperature were recorded with a Seabird® SBE 911 Conductivity–Temperature–Depth/pressure (CTD) sensor package. Discrete water samples were collected at selected stations with 20-L Go-Flo bottles mounted on a Rosette sampler. Following the protocols of the best practices for measuring the ocean carbonate system parameters (Dickson et al., 2007), subsamples for C_T, A_T and pH measurements were taken with Tygon® tubing free of air bubbles, with ample sample overflow in order to minimize any contamination from atmospheric CO_2. Samples for C_T, and A_T measurements were taken into 500 mL borosilicate bottles and poisoned with a saturated $HgCl_2$ solution. The samples were stored in the dark and returned to a land-based laboratory for analyses within one and two months of sample collection for C_T and A_T, respectively. pH samples were taken into 10 cm optical cells. pH measurements were made onboard the ship within two hours of sample collection.

Please cite this article as: Guo, X., Wong, G.T.F., Carbonate chemistry in the Northern South China Sea Shelf-sea in June 2010. Deep-Sea Res. II (2015), http://dx.doi.org/10.1016/j.dsr2.2015.02.024

Analyses of C_T and A_T followed the methods in Cai et al. (2004). C_T was measured by collecting and quantifying the CO_2 released from the sample upon acidification with a non-dispersive infrared detector (Li-Cor® 7000) using an Apollo SciTech model AS-C3 DIC Analyzer. The analyzer was calibrated with the certified reference materials (CRM) provided by Dr. A.G. Dickson of the Scripps Institution of Oceanography. Additionally, eighty CRM measurements were inserted randomly into the work-stream during the analyses of the field samples, and each was analyzed at least in triplicate. The resulting average precision in the repeated analyses of these quality-control samples was better than $\pm 0.1\%$ and the average deviation from the expected values was 1.4 μmol kg^{-1}.

A_T was determined by a Gran titration with hydrochloric acid using an automated alkalinity titrator (Apollo SciTech model AS-ALK2). The acid was standardized with the CRM. After every 20 field samples were analyzed, the CRM was inserted into the work-stream and analyzed as a sample. The CRM was thus analyzed for 20 times during the sample analyses. The precision estimated from these repeated analyses was ± 1.8 μmol kg^{-1}. The average deviation from the expected value was 2.0 μmol kg^{-1}.

Samples for pH measurements were placed in a constant temperature bath at 25 ± 0.01 °C for about 1 h before their pH values were measured spectrophotometrically at the same temperature in a thermostated cell with a Perkin Elmer Model Lambda 35 UV/vis spectrophotometer, using m-cresol purple sodium salt (Sigma-Aldrich) as the indicator (Dickson et al., 2007). Correction for indicator perturbation was made following the procedure of Dickson et al. (2007). The precision of the measurement was ± 0.0008 pH unit when a sample of aged seawater was analyzed 14 times in the laboratory before the cruise. Correction for indicator impurity was not made as the procedure (Liu et al., 2011) was not available during this work. A subsequent comparative study of eight replicates of four samples of aged seawater, with a pH range of 7.58–8.16, indicated that the pH values obtained by using the indicator used in this study were 0.0049 ± 0.0006, with a range of 0.0045–0.0056, lower than the values determined when a purified indicator, obtained from Dr. Robert Byrne (University of South Florida), was used. These results indicate that the effect from indicator impurity was significant relative to the precision, ± 0.0008, of the pH measurements but the offset was quite consistent.

Nutrient samples were drawn into high-density polyethylene bottles. Samples for the determination of soluble reactive phosphorus (SRP) were quickly frozen with liquid nitrogen and stored at −20 °C and then returned to a land-based laboratory for analysis. SRP was determined manually by the standard phospho-molybdate blue method (Strickland and Parsons, 1972) at a precision of ± 0.01 μmol L^{-1} or $\pm 3\%$, whichever was greater. For the determination of silicate, the samples were stored refrigerated at 5 °C until they were analyzed manually by the standard reduced silico-molybdate blue method (Strickland and Parsons, 1972). The precision of the measurement was $\pm 3\%$.

2.3. Data processing

In situ aragonite saturation state (Ω_{Ar}), partial pressure of CO_2 (pCO_2) and *in situ* pH were calculated from C_T and A_T using the program CO2SYS (Pierrot et al., 2006). The dissociation constants of carbonic acid were taken from Mehrbach et al. (1973) as refitted by Dickson and Millero (1987). CO_2 solubility coefficient was taken from Weiss (1974) and the bisulfate dissociation constant from Dickson (1990). The concentrations of SRP and silicate were also used in these calculations. The $CaCO_3$ solubility products were calculated using the equations of Mucci (1983).

Normalized A_T and C_T at a reference salinity of 34.0 were calculated following the scheme of Friis et al. (2003) such that:

$$NX = \frac{X^{obs} - X^{S=0}}{S^{obs}} \times 34 + X^{S=0} \quad (1)$$

in which, X is A_T or C_T, and X^{obs} and S^{obs} are the observed A_T or C_T, and salinity, respectively. $A_T^{S=0}$ is the intercept in the linear regression analysis of A_T against salinity down to a depth of 150 m or the sea bottom if the water depth of the station was shallower than 150 m. $C_T^{S=0}$ is the intercept in the linear regression analysis of C_T against salinity in the mixed layer. Only the data in the mixed layer were use in the latter case because the relationship between C_T and salinity became non-linear at greater depths. The mixed layer depth was defined as the depth at which the potential density gradient reached or exceeded 0.1 m^{-1} (Green et al., 2006; Tseng et al., 2005). A salinity of 34.0 was used as it was approximately the average salinity in the mixed layer.

pCO_2 was normalized to a temperature of 27 °C ($NpCO_2$) using the following equation (Takahashi et al., 2002):

$$NpCO_2 = pCO_2 \times \exp[27 - sst] \quad (2)$$

where sst is the sea surface temperature. A temperature of 27 °C was used as it corresponded approximately to the average temperature in the mixed layer.

The value of pH at *in situ* temperature (*in situ* pH) was calculated from C_T and pH_{25} using the program CO2SYS (Pierrot et al., 2006) with the same constants as those in the Ω calculation. To gauge the internal consistency of the measurements in the carbonate system, we calculated A_T from pH_{25} and C_T with the program CO2SYS. The differences between the calculated and measured A_T ranged between 0.0 and 9.4 μmol kg^{-1}, with an average of 3.9 ± 2.2 μmol kg^{-1}. Given that the analytical precision in the measured A_T was about ± 2 μmol kg^{-1} and that there was also uncertainty in the calculated A_T, this average difference was considered acceptable and it indicated a reasonable degree of internal consistency, if not accuracy, in the measurements.

Net CO_2 flux (F_{CO_2}) between the surface water and the atmosphere was calculated with the following formula:

$$F_{CO_2} = k \times s \times \Delta pCO_2 \quad (3)$$

where s is the solubility of CO_2 (Weiss, 1974), ΔpCO_2 is the pCO_2 difference between the surface water and the atmosphere; and k is the CO_2 gas transfer velocity between the surface water and the atmosphere. Gas transfer velocity was parameterized using the empirical function of Sweeney et al. (2007) and Ho et al. (2006) such that

$$k = 0.27 \times U_{10}^2 \times (Sc/660)^{-0.5} \quad (4)$$

where U_{10} is the wind speed at 10 m above sea level and Sc is the Schmidt number at the *in situ* temperature in the seawater (Wanninkhof, 1992). The wind speed data, at a resolution of $2.5° \times 2.5°$, were obtained from the National Center for Environmental Prediction of the United States. The arithmetic average wind speed from June 3 to 12 in the study area was adopted in the calculation. Atmospheric pCO_2 (pCO_2^{atm}) was calculated from the CO_2 fraction (xCO_2) in the atmosphere at the Dongsha Island and the barometric pressure (P) after correcting for the water vapor pressure (P_{H_2O}) (Weiss and Price, 1980):

$$pCO_2^{atm} = (P - P_{H_2O}) \times xCO_2 \quad (5)$$

The average air xCO_2 at Dongsha Island during the cruise (393.2 ppm, Global Monitoring Division, Earth System Research Laboratory, National Oceanic & Atmospheric Administration, data available at http://www.esrl.noaa.gov/gmd/dv/data) was adopted in the calculation. As defined here, a positive flux indicates an evasion of CO_2 from the sea to the air. The average CO_2 flux was the

Please cite this article as: Guo, X., Wong, G.T.F., Carbonate chemistry in the Northern South China Sea Shelf-sea in June 2010. Deep-Sea Res. II (2015), http://dx.doi.org/10.1016/j.dsr2.2015.02.024

arithmetic average of the stations where net community production, NCP, was calculated.

3. Results and discussion

3.1. Hydrographic characteristics

The relationship between potential temperature and salinity (Fig. 3) indicates that the water masses in the study area include the surface water, the North Pacific Tropical Water (NPTW), the North Pacific Intermediate Water (NPIW) and the North Pacific Deep Water. The NPTW and NPIW are represented by the salinity maximum at 100–150 m and the salinity minimum at 400–450 m. This water mass structure is similar to that reported previously in the open northern SCS basin (Chou et al., 2007).

The distributions of temperature and salinity in the surface waters and along each of the cross-shelf transects are shown in Figs. 4 and 5. A more detailed discussion on the hydrographic conditions during this study and the climatology of the hydrographic characteristics in the study area is found elsewhere in this special issue (Wong et al., this issue-b) and is only briefly summarized here. The study area may be sub-divided into the inner shelf, the middle shelf, the outer shelf and the open northern SCS at water depths of <40, 40–90, 90–200 and >200 m, respectively. The mixed layer depth during this cruise, $\sim$40 m, was similar to those found during the summer in previous studies (Cai et al., 2004; Cao et al., 2011; Wong et al., 2007). The mixed layer was underlain by a relatively homogenous layer of sub-surface water that extended into the NoSoCS from the open northern SCS. In the inner shelf, the water column was vertically well mixed. The temperature and salinity were lower while the concentration of chlorophyll *a* (not shown here) was higher than those in the waters in the surface mixed layer further offshore. In contrast, the hydrographic characteristics on the outer shelf approached those in the open northern SCS, where the water was warm and saline and the chlorophyll *a* concentration was low. Superimposed on these sub-regions was the effect of offshore upwelling between Shanwei and Shantou, a phenomenon that has been reported to occur in this area (Gan et al., 2009a). This was indicated by the coastward and upward-tilting isopleths of temperature and salinity in transect T1 (Fig. 5A-4 and B-4) and by the associated patch of exceptionally cold and saline surface water (Fig. 4A and B). The presence of the saline upwelling water actually resulted in a higher salinity in the inner shelf than further offshore off the coast of Shantou (Fig. 5A-4). Evidence for the activity of internal waves, which was indicated by the undulating isohalines and isotherms at the bottom of the mixed layer, was present along the entire shelf (Fig. 5A-1–A-4). These internal waves extended shoreward from the open northern SCS to at least the middle shelf, and their effects were most prominent in the outer shelf (Chang et al., 2011; Li et al., 2008; Pan et al., 2012). The slightly elevated salinities in the outer shelf, especially around Dongsha Atoll where some of the strongest internal waves in the world are found (Chang et al., 2006; Hsu et al., 2000; Wang et al., 2007), relative to the water either further offshore and onshore, could be related to the enhanced entrainment by these waves of saline sub-surface water to the surface mixed layer.

A parcel of anomalously lower salinity water was found at the coast in the northwestern corner of the study area off Maoming

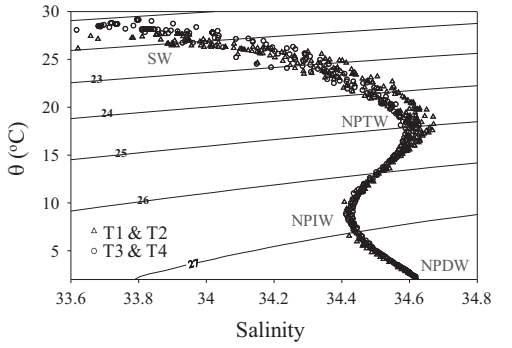

Fig. 3. *T–S* (potential temperature vs. salinity) relationships at all the stations. SW – surface water; NPTW – North Pacific Tropical Water; NPIW – North Pacific Intermediate Water; and NPDW – North Pacific Deep Water.

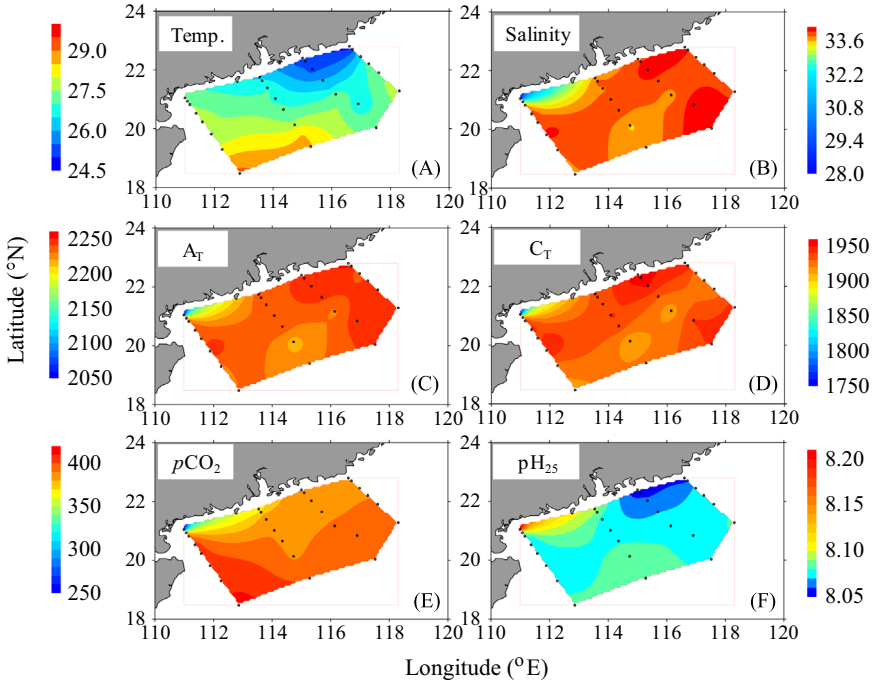

Fig. 4. Surface distributions of (A) temperature (Temp., °C), (B) salinity, (C) A_T (μmol kg^{-1}), (D) C_T (μmol kg^{-1}), (E) pCO_2 (μatm) and (F) pH_{25}. The open circles are the sampling stations.

Please cite this article as: Guo, X., Wong, G.T.F., Carbonate chemistry in the Northern South China Sea Shelf-sea in June 2010. Deep-Sea Res. II (2015), http://dx.doi.org/10.1016/j.dsr2.2015.02.024

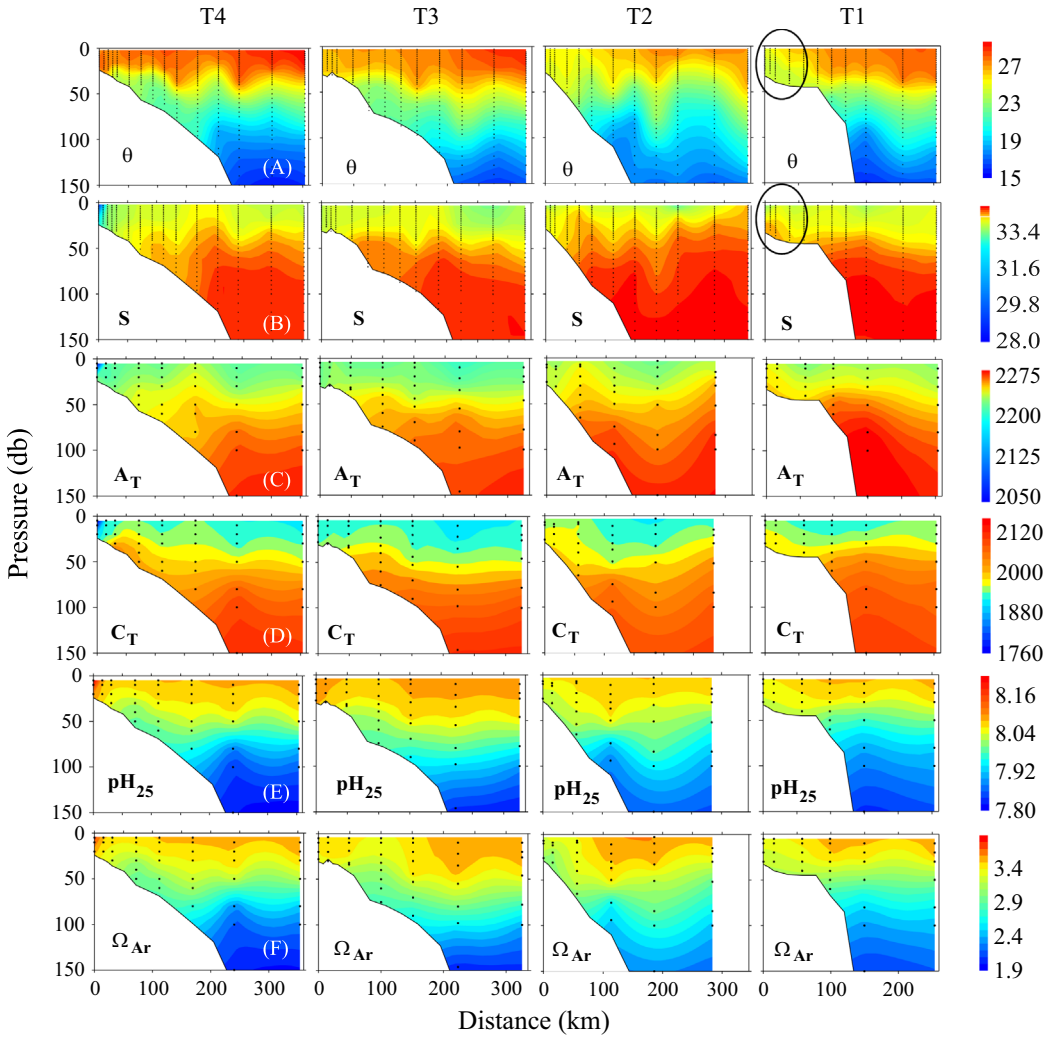

Fig. 5. Depth distributions of (A) potential temperature (θ, °C), (B) salinity (S), (C) A_T (μmol kg^{-1}), (D) C_T (μmol kg^{-1}), (E) pH_{25}, and (F) Ω_{Ar} along transects T1–T4. "Distance" denotes the distance from the most inshore station. Circles in sections in temperature and salinity in transect T1 – indications of upwelling by upward tilting isotherm and isohalines towards the coast.

where salinities dropped abruptly to <30 (Fig. 4B). The source of this water is uncertain. Submarine ground water and local river discharges outside the sampling area are both possibilities. Except for this water parcel, salinity fell within a narrow range of 33.6–34.2. The presence of the Pearl River plume, which should be represented as a patch of lower salinity water off the mouth of the river, was not prominent. This might reflect the fact that the sampling period in this study just preceded the arrival of the high flow from the river and followed an exceptionally dry spring, since the discharge of the Pearl River in March–May, 2010 was ~30% lower than the long-term average (Fig. 2).

3.2. Distributions of A_T, C_T, pCO_2 and pH_{25}

3.2.1. Surface distributions

Surface distributions of A_T, C_T, pCO_2 and pH_{25} are shown in Fig. 4. A_T fell within 2210–2250 μmol kg^{-1} (Fig. 4C) excluding in the exceptionally lower salinity water off Maoming where A_T dropped to <2100 μmol kg^{-1}. The pattern of distribution followed that of salinity closely, with higher A_T generally corresponding with higher salinity. The pattern of C_T distribution was also similar to that of salinity but the correlation was not as strong as that of A_T (Fig. 4D). Thus, higher C_T was generally associated with the more saline water in the upwelling area and around the Dongsha Atoll and the lowest C_T (<1800 μmol kg^{-1}) was found in the lowest salinity water off Maoming. However, the highest C_T did not co-locate with the highest salinity off Shantou but was found off Shanwei. Except for the water off Maoming, C_T ranged between 1910 and 1960 μmol kg^{-1} (Fig. 4D).

Surface pCO_2 ranged between 362 and 413 μatm, except at off the coast of Maoming, where it dipped to <260 μatm. The pCO_2 in surface seawater were generally higher than that in the atmosphere (~390 μatm), and waters with pCO_2 below the atmospheric pCO_2 levels were confined only to the coastal waters off Maoming and the Pearl River estuary (Fig. 4E). The distributional pattern of pCO_2 generally resembled that of temperature such that higher pCO_2 was found in warmer water. Thus, pCO_2 increased seaward as the temperature became higher, except in the upwelling water off Shanwei and Shantou where pCO_2 was high but temperature was low.

Excluding the water off Maoming, surface pH_{25} fell between 8.05 and 8.09. Its distributional pattern was similar to that of temperature so that the lower values, <8.07, were generally found in the colder upwelling water off Shantou and Shanwei while the higher values, >8.08, tended to appear in the warmer water offshore. Off Maoming, surface pH_{25} rose to >8.2, the highest value found in the NoSoCS (Fig. 4F).

Please cite this article as: Guo, X., Wong, G.T.F., Carbonate chemistry in the Northern South China Sea Shelf-sea in June 2010. Deep-Sea Res. II (2015), http://dx.doi.org/10.1016/j.dsr2.2015.02.024

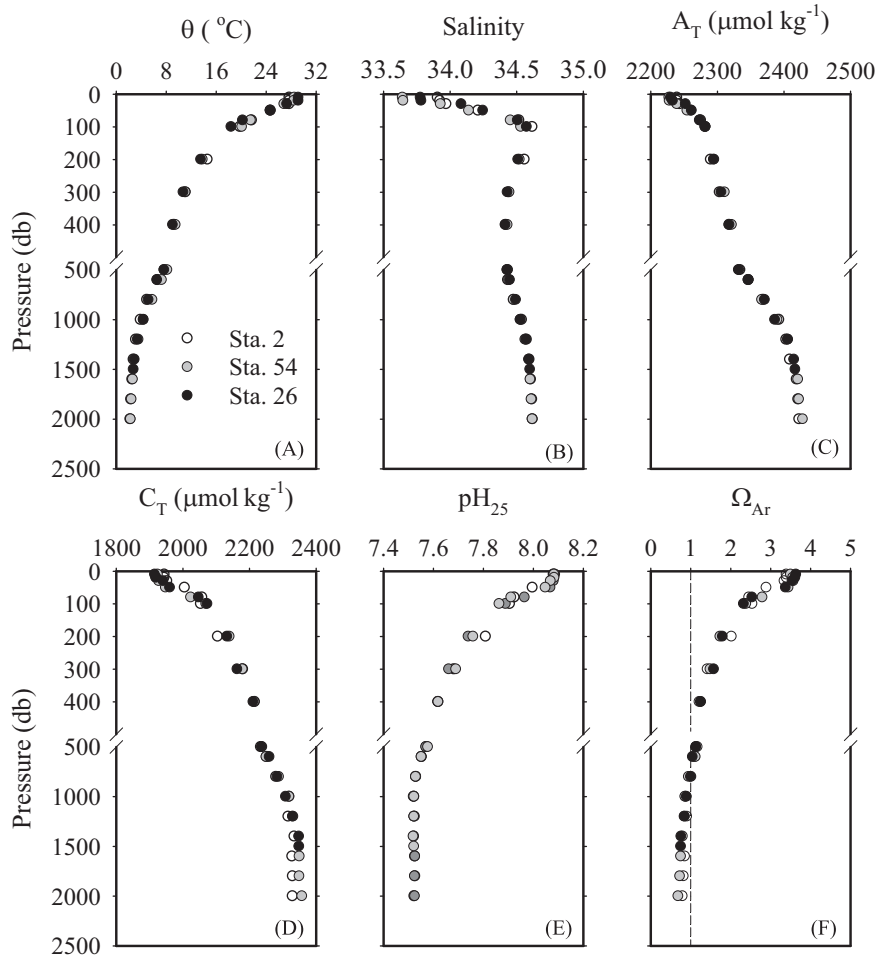

Fig. 6. Vertical distributions of (A) potential temperature (θ), (B) salinity, (C) A_T, (D) C_T, (E) pH_{25}, and (F) Ω_{Ar} at Stations 2, 26 and 54 stretching along the length of the seaward edge of the NoSoCS (Fig. 1). They are the only stations occupied with water depths exceeding 1500 m and are used to represent the conditions in the open northern SCS. Dotted line in (F) denotes $\Omega_{Ar}=1$.

3.2.2. *Vertical distributions*

With depth, A_T and C_T increased steadily below the mixed layer to about 2425 and 2335 μmol kg^{-1}, respectively, below 1500 m (Fig. 6). The pH_{25} values decreased with depth. At the bottom of the mixed layer at around 40 m, pH_{25} approached 8.0 (Fig. 5E). Below the mixed layer, pH_{25} continued to drop conspicuously to 7.8–7.9 at 150 m at the core of the NPTW and to 7.5 at >1500 m (Fig. 6E). There was a distinct undulation in the isopleths of pH_{25} below the mixed layer in transect T2 as a result of the enhanced vertical mixing by internal waves, and waters with lower pH_{25} were able to reach shallower depths (Fig. 5E-3).

The distributional patterns of the carbonate species reported here are somewhat different from those reported previously (Cao et al., 2011). Waters with low salinity, C_T and A_T, which are indicative of riverine input, were conspicuously absent in the middle shelf and in most of the inner shelf in the absence of a significant Pearl River plume during this study, in contrast to prior studies by Cai et al. (2004) and Cao et al. (2011).

3.3. *Physical and biological controls on the carbonate system*

The similarity in the surface distributions of A_T and salinity suggests that physical mixing is the primary process controlling the distribution of A_T. Indeed, data from the upper 150 m yield a strong linear relationship (Fig. 7A) such that

$$A_T(\mu\text{mol kg}^{-1}) = 62.6(\pm 1.0) \times S + 116(\pm 35) \quad N = 159, \quad R^2 = 0.96 \qquad (6)$$

where S is salinity, R is the correlation coefficient and N is the number of data points. At a salinity of 34.6 (the average salinity at the core of the NPTW), this relationship yields a A_T of 2282 μmol kg^{-1}, which is quite similar to the previously reported values (Tseng et al., 2007). Thus, A_T in the NoSoCS is primarily controlled by mixing between the saline sub-surface NPTW and the fresher surface water whose composition may be influenced by riverine input, submarine groundwater discharge and atmospheric precipitation. In contrast, although a linear relationship is also found in the open northern SCS, the intercept is virtually zero (Tseng et al., 2007). This indicates that the fresh water end-member in the open SCS is probably rain-water. The influence from terrestrial sources, which may be high in A_T, is minimal. The large positive intercept in the relationship between A_T and salinity in the NoSoCS is indicative of the influence of mixing with terrestrial sources of fresh water containing considerable A_T as the A_T in Pearl River water during a similar time period of the year and in submarine ground water discharge to the region have been reported to be 1190 μmol kg^{-1} (Guo et al., 2008) and 4020 μmol kg^{-1} (Liu et al., 2012) respectively. In fact, when the dataset is further subdivided into waters in the NoSoCS proper (water depth <130 m) and in the inner shelf alone (water depth <40 m) in

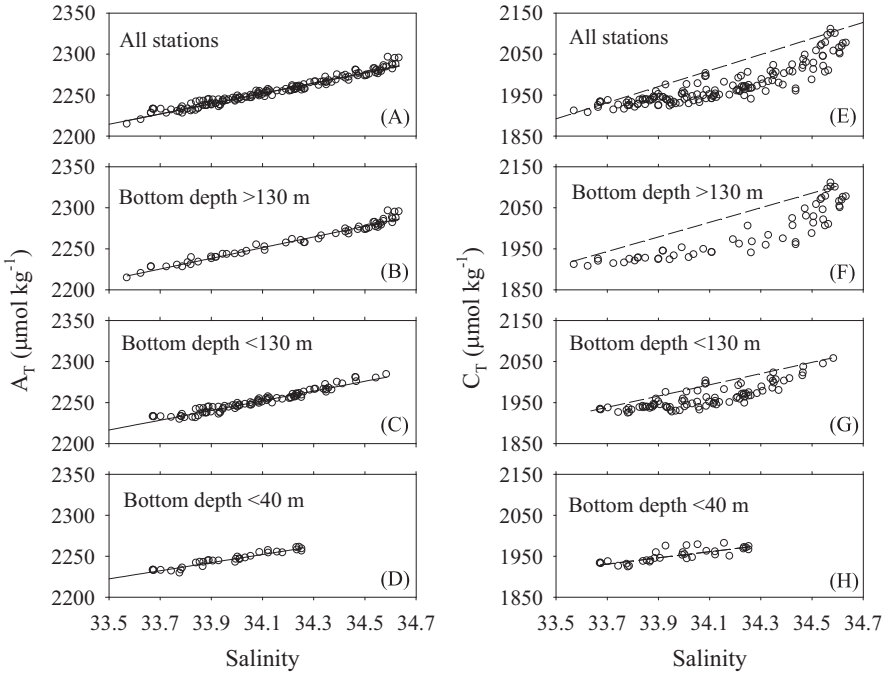

Fig. 7. Relationships between A_T and salinity (S) and between C_T and salinity (S) in the upper 150 m in (A and E) the entire study area; (B, F) the open Northern South China Sea Shelf-sea (NoSoCS) beyond the shelf-break (bottom depth >130 m); (C and G) the NoSoCS shelf (bottom depth <130 m); and (D and H) the inner shelf (bottom depth <40 m). Solid lines in A–D – linear regression lines; dashed lines in E–H – hypothetical mixing lines.

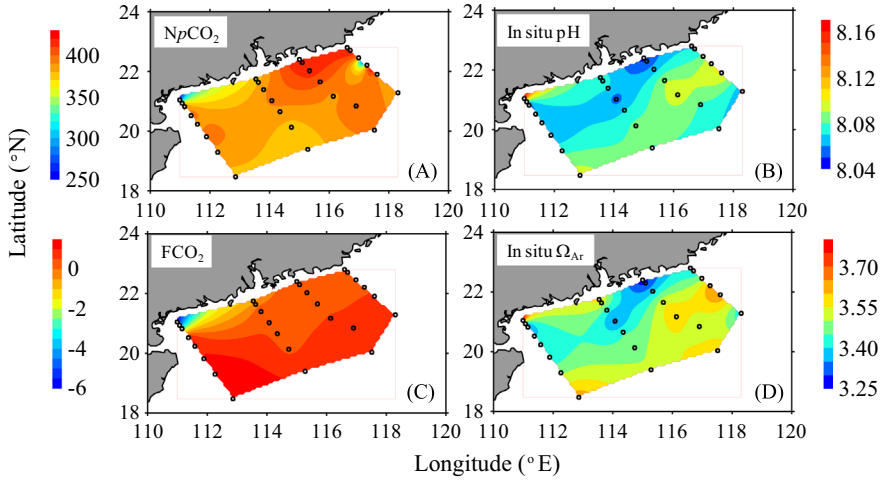

Fig. 8. Surface distributions of (A) pCO_2 normalized to 27 °C (NpCO_2, μatm), (B) *in situ* pH, (C) CO_2 flux (FCO_2, mmol m^{-2} d^{-1}) and (D) *in situ* Ω_{Ar}. The open circles are the sampling stations.

order to detect the larger terrestrial influence in the inner shelf the relationships becomes, respectively:

For water depth <130 m (Fig. 7C)

$$A_T(\mu\text{mol kg}^{-1}) = 59.4(\pm 1.5) \times S + 227(\pm 52) \quad N = 99, \quad R^2 = 0.95 \tag{7}$$

For water depth <40 m (Fig. 7D)

$$A_T(\mu\text{mol kg}^{-1}) = 49.4(\pm 2.4) \times S + 567(\pm 82) \quad N = 43, \quad R^2 = 0.93 \tag{8}$$

While the linearity of the A_T versus salinity relationship is maintained, the slope becomes progressively smaller and the intercept becomes progressively larger as the waters are increasingly influenced by terrestrial inputs. Nevertheless, since the samples were collected during a period of low flow, the effect of terrestrial inputs was probably not at its maximum.

When A_T is normalized to a constant salinity of 34.0 (the average salinity in the upper 150 m in the NoSoCS), the resulting NA_T ranges between 2240 and 2256 μmol kg^{-1} and the average is 2246 (± 3) μmol kg^{-1}. The standard deviation of the average value, ± 3 μmol kg^{-1}, is similar to the analytical uncertainty of ± 2 μmol kg^{-1}. This quasi-conservative behavior of A_T suggests that, while the removal of calcium carbonate through calcification should be a common occurrence in the abundant coral reef ecosystems in the NosSoCS (Guo et al., 1994) and other processes (such as $CaCO_3$ dissolution and anaerobic respiration) may also take place and affect A_T, the combined effect of these processes is not large enough to be detected in the NoSoCS as a whole.

Unlike A_T, the relationship between C_T and salinity in the upper 150 m of the water column (Fig. 7E) is prominently curvilinear.

Please cite this article as: Guo, X., Wong, G.T.F., Carbonate chemistry in the Northern South China Sea Shelf-sea in June 2010. Deep-Sea Res. II (2015), http://dx.doi.org/10.1016/j.dsr2.2015.02.024

A similar pattern has been reported previously in the open northern SCS (Tseng et al., 2007). The concavity in the relationship indicates non-conservative behavior and suggests that C_T is removed from the NoSoCS and that the distribution of C_T is not controlled by mixing alone. Two obvious processes that might contribute to the removal are the net evasion of CO_2 to the atmosphere and net community production (NCP). This pattern is similar to that previously reported in the open northern SCS (Tseng et al., 2007).

The range of NpCO_2 in the surface waters (371–425 µatm except for the lower salinity water off Maoming) was quite similar to that of pCO_2 (362–413 µatm), while the distributional patterns of the two were distinct from each other (Figs. 8A and 4E) indicating that, aside from temperature changes, other processes, such as mixing between water masses, respiration and photosynthesis, also likely contribute to the variations in pCO_2 in these productive shelf-waters. In most of the middle and outer shelf, although NpCO_2 fell within a narrow range (~390 µatm), the corresponding *in situ* pCO_2 was decidedly higher, frequently exceeding 400 µatm (Fig. 4E). In these waters, temperature change as a result of summer heating is a likely major cause of the higher pCO_2. However, even then, while pCO_2 is significantly positively correlated with sea surface temperature (Fig. 9A) such that

$$pCO_2 = 5.5(\pm 1.5) \times sst + 244(\pm 41)$$
$$N = 25, \quad R^2 = 0.36, \quad p = 0.0015 \tag{9}$$

where sst is sea surface temperature in °C, the correlation coefficient is low and is much lower than those previously reported for the open northern SCS basin (Tseng et al., 2007).

In the inner shelf off Shanwei and Shantou, the effect of upwelling was clearly captured in the distribution of NpCO_2. A moderately high pCO_2 turned into the highest NpCO_2 (410–430 µatm) in the study area (Fig. 8A), as cold sub-surface water with elevated pCO_2 (as a result of the oxidation of organic matter) found its way to the surface mixed layer. In the coastal water off Maoming, distinctly lower salinity, A_T and C_T, and higher pH were found and they were accompanied by the lowest pCO_2 observed in the NoCoCS (Fig. 4E). The origin of this water could not be identified definitively from the present data-set. Local sources of freshwater, such as the inflow from the Jianjiang River, is a possibility but the composition of these waters is not yet well documented. Discharge from the Pearl River and groundwater discharge could account for the lower salinity but not the lower A_T as it is elevated in these waters (Guo et al., 2008; Liu et al., 2012). Photosynthetic activities could also have contributed to the lower pCO_2, NpCO_2, C_T and higher pH_{25} but they could not account for the lower salinity and A_T. In the vicinity of the Dongsha Atoll, both pCO_2 and NpCO_2 were moderately high, ~400 µatm. The high NpCO_2, salinity, A_T and C_T were consistent with the enhanced entrainment of the subsurface water with high pCO_2 into the mixed layer by internal waves or eddies (Chow et al., 2008; Wang et al., 2007).

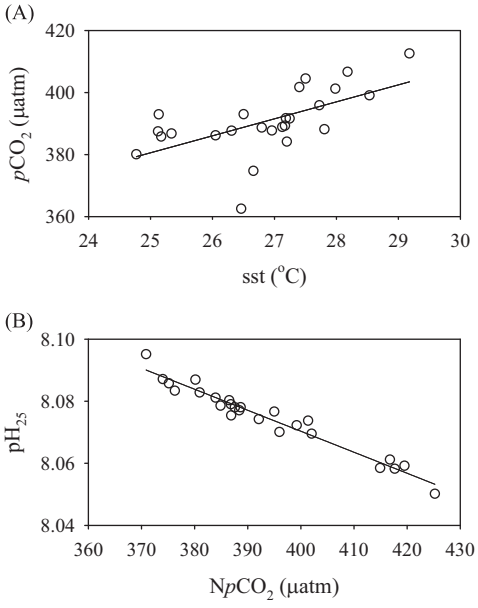

Fig. 9. Relationships between (A) pCO_2 and sea surface temperature (sst); and (B) pH_{25} and NpCO_2.

As expected from the thermodynamics of the carbonate system, surface pH_{25} is negatively correlated to NpCO_2

$$pH_{25} = -6.8(\pm 0.3) \times 10^{-4} \times NpCO_2 + 8.341(\pm 0.013)$$
$$N = 25, \quad R^2 = 0.95, \quad p < 0.0001 \tag{10}$$

As a result, the distribution of NpCO_2 resembles an inverse of that of pH_{25} (Figs. 4D and 8A) and processes controlling NpCO_2 would also have affected pH_{25}.

3.4. Biogeochemical dynamics of the carbonate system – biological uptake of C_T

In the study area, the linear relationship between A_T and salinity in the upper 150 m (Fig. 7A) indicates that the mixed layer might be approximated as the result of a two end-member mixing between the fresher surface water and the sub-surface NPTW. If a steady state in the carbonate system is assumed, the C_T deficit ($C_{T,def}$) relative to conservative mixing (Fig. 7E) can be attributed to the loss of C_T through evasion of CO_2 to the atmosphere and its biological uptake during photosynthesis. Thus,

$$\delta(C_{T,def})/\delta t = (\Delta C_T \times Z)/\tau = NCP + F_{CO_2} \tag{11}$$

where t is time, ΔC_T is the average deficit in C_T in the mixed layer with a thickness of Z, τ is the residence time of the mixed layer water, NCP is the net community production and F_{CO_2} is the evasion flux of CO_2 to the atmosphere. Since ΔC_T, Z and F_{CO_2} can be estimated from the observed distribution of the carbonate species and the hydrographic characteristics, and estimations of τ have been reported previously, NCP may then be calculated.

The NPTW can be represented by the salinity maximum of 34.62 ± 0.05 (Fig. 3; Wong et al., this issue-b). A similar salinity is found in NPTW at the nearby SouthEast Asian Time-series Study (SEATS) station (Wong et al., 2007). The salinity of the surface water may be estimated to be about 33.68(±0.07) from the relationship between A_T and salinity in the NoSoCS (Fig. 7C). The corresponding A_T and C_T in these two end members may then be estimated at these two salinities and their compositions are listed in Table 1. The expected C_T under conservative mixing may then be calculated at any given intermediate salinity from the composition of these two end members and ΔC_T, defined as the difference between the measured C_T and the expected C_T from conservative mixing, may also be calculated. The average ΔC_T in the mixed layer in the study area is estimated to be −36 (±31) µmol kg^{-1}. The thickness of the mixed layer in this study is 40 (±10) m. Cai et al. (2004) estimate τ in the mixed layer in the adjacent northern SCS to be one year. The average basin wide upwelling rate in the SCS is reported to be between 10 and 90 m y^{-1} (Wong et al., 2007), but a

Table 1
End-member values in the non-conservative C_T calculation.

End-member	Salinity	C_T (µmol kg^{-1})	A_T (µmol kg^{-1})
Surface water	33.67 (±0.07)	1921.8 (±9.2)	2227.0 (±7.4)
Sub-surface water	34.62 (±0.05)	2067.9 (±10.8)	2288.1 (±5.5)

Please cite this article as: Guo, X., Wong, G.T.F., Carbonate chemistry in the Northern South China Sea Shelf-sea in June 2010. Deep-Sea Res. II (2015), http://dx.doi.org/10.1016/j.dsr2.2015.02.024

recent study (Qu et al., 2006) favors the higher value. The upwelling rate in the NoSoCS, which covers most of the study area, is likely to be even higher as a result of the additional processes that enhance vertical mixing, such as coastal upwelling and the action of internal waves (Chang et al., 2011; Gan et al., 2009a). Hence, the maximum value of 90 ($\pm$50) m y^{-1} is used. The corresponding τ is 0.4 $\pm$ 0.8 y, with a range of 0.3–1.0 y. The resulting rate of change of $C_{T,def}$ is 10.0 $\pm$ 19.9 mmol C m^{-2} d^{-1}, with a range of 4.0–13.3 mmol C m^{-2} d^{-1}. Since the average efflux of CO_2 is estimated to be 0.5 ($\pm$0.5) mmol C m^{-2} d^{-1}, NCP would then be 9.5 $\pm$ 19.9 mmol C m^{-2} d^{-1}, with a range of 3.5–12.8 mmol C m^{-2} d^{-1}. Thus, NCP is the primary contributor to the deficit in C_T.

In comparison, Cai et al. (2004) report a rate of 10–14 mmol C m^{-2} d^{-1} in July 2000 during a non-bloom period in the NoSoCS off the Pearl River mouth. During a bloom period, a higher value is expected and Cao et al. (2011) estimate a rate of 36 mmol C m^{-2} d^{-1} in July 2008 in the northern half of the NoSoCS. The average new production in the shelf and the slope of the northern SCS are estimated to be 5–14 mmol C m^{-2} d^{-1} (Chen and Chen, 2006). The export flux of particulate organic carbon in the northern SCS is reported to be 0.5–12.1 mmol C m^{-2} d^{-1} (Chen et al., 2008). Given the large uncertainties in the reported estimations, the value we obtained agrees reasonably well with the range of previously reported values.

Gan et al. (2009b) suggest that summer coastal upwelling at the northeastern corner of the NoSoCS starts off Shanwei. The upwelling water spreads northeastward and does not outcrop at the surface until it reaches Shantou. A comparison of the hydrographic and biogeochemical characteristics at the stations closest to the coast along transect T2 off Shanwei with those of transect T1 off Shantou is consistent with this suggestion. Surface temperature was lower while salinity was higher in transect T1, suggesting that the effect of upwelling of the cold and more saline sub-surface water was more prominent in this transect (Fig. 10A and B). Concomitantly, while surface A_T was higher and C_T was slightly lower in transect T1 (Fig. 10C and D), once the effect of the salinity change was removed, surface NA_T became about the same in both transects while NC_T remained decidedly lower in T1 (Fig. 10E and F). These trends are consistent with a higher rate of carbon uptake by biological production in the upwelled water in transect T1. The difference in NC_T in the mixed layer at the coastal stations between the two transects is -15.9 ± 7.8 µmol kg^{-1}. The average mixed layer depth at these stations is 13.2 ($\pm$3.2) m. Therefore, the integrated C_T removal in the mixed layer is 214 ($\pm$117) mmol C m^{-2}. If the water residence time in the upwelling area along transect T1 is assumed to be the same (7 days) as that estimated in the summer of 2008 (Cao et al., 2011), the C_T removal rate would be 30.6 ($\pm$16.8) mmol C m^{-2} d^{-1}. The air–sea exchange flux of CO_2 in this area is 0.3 ($\pm$0.2) mmol C m^{-2} d^{-1}. Again assuming that the removal of C_T in the mixed layer is sustained by air–sea exchange and NCP (Eq. (11)), NCP in the upwelling water off Shantou in transect T1 would be 30.3 ($\pm$16.8) mmol C m^{-2} d^{-1}. This NCP is more than twice the average value, 9.5 mmol C m^{-2} d^{-1}, of the NoSoCS but is similar to the value of 36.0 mmol C m^{-2} d^{-1} reported for this upwelling zone in July 2008 (Cao et al., 2011). Higher NCP in the upwelling zone relative to the NoSoCS as a whole is consistent with what might be expected. Nevertheless, the estimated rates should be taken with some caution as the assumptions involved in the calculation need to be further validated.

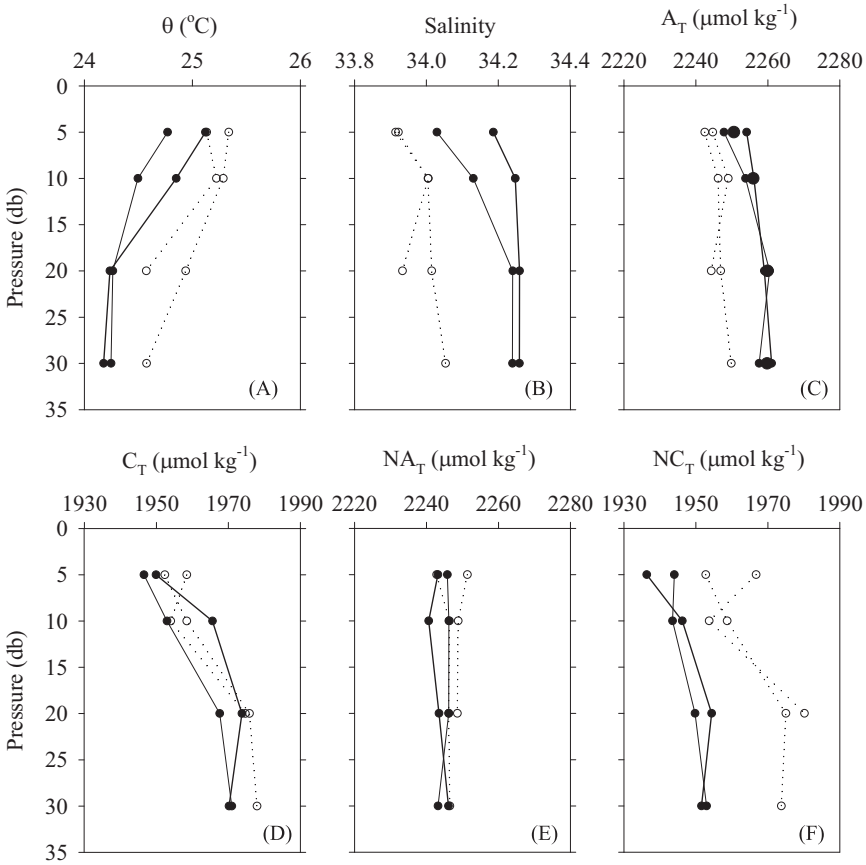

Fig. 10. Comparisons of the vertical distributions of (A) potential temperature (θ); (B) salinity; (C) A_T; (D) C_T; (E) NA_T; and (F) NC_T at the two most coastal stations in transects T1 and T2. • – transect T1; ○ – transect T2.

Please cite this article as: Guo, X., Wong, G.T.F., Carbonate chemistry in the Northern South China Sea Shelf-sea in June 2010. Deep-Sea Res. II (2015), http://dx.doi.org/10.1016/j.dsr2.2015.02.024

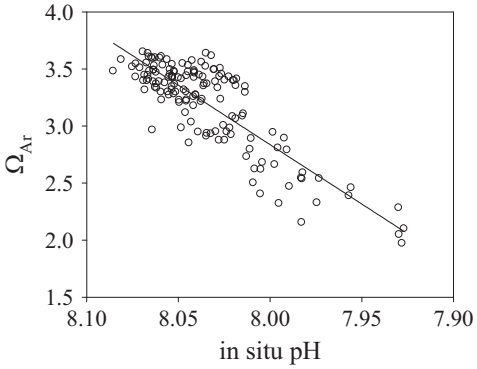

Fig. 11. Relationship between the aragonite saturation state (Ω_{Ar}) and *in situ* pH in the upper 150 m. The solid line is the linear regression line.

3.5. The aragonite saturation state, Ω_{Ar}, and tropical shallow water corals

The surface water was invariably super-saturated with respect to aragonite ($\Omega_{Ar} > 1$) but Ω_{Ar} never exceeded 3.8 (Fig. 8D). In most area, surface Ω_{Ar} was around 3.3–3.5. In the inner shelf, it dropped to 3.2 in the upwelling water and rose to 3.8 in the isolated parcel of lower salinity water off Maoming. Ω_{Ar} decreased with depth and dropped below 3.0 at about 50 m and to 2.0 at about 140 m (Fig. 5F). Upwelling brought waters with lower Ω_{Ar} to shallower depths in the inner shelf in transects T1 and T2. The action of internal waves in the outer-shelf resulted in the undulation of the isopleths in Ω_{Ar}. Beyond the shelf break, surface Ω_{Ar} increased slightly to 3.5–3.7 (Fig. 8D). With depth, Ω_{Ar} decreased to 1.0 at 600–800 m and to 0.8 at 2000 m (Fig. 6F). These values are similar to those reported for the open northern SCS basin (Chou et al., 2007) and the nearby northwest Pacific (Feely et al., 2002). Kleypas et al. (1999b) and Guinotte et al. (2003) suggest that waters with values of Ω_{Ar} between 3.0 and 3.5 may be considered "marginal" and below 3.0 may become "extremely marginal" for the growth of most coral reefs. Under this scheme, the condition of surface Ω_{Ar} in most of the NoSoCS has entered the "marginal" range. Nevertheless, it should be noted that calcifying/accreting corals have been observed recently in waters with Ω_{Ar} values of at least as low as 2.8 (Shamberger et al., 2011).

The Ω_{Ar} in the NoSoCS is linearly related to *in situ* pH, pH_{is}, (Fig. 11) such that

$$\Omega_{Ar} = 10.4042(\pm 0.5496) \times pH_{is} - 80.3966(\pm 4.4160)$$

$$N = 150, \quad R^2 = 0.71, \quad p < 0.0001 \qquad (12)$$

Thus, at a Ω_{Ar} of 3.0, when the condition becomes "extremely marginal" for coral growth according to the scheme of Kleypas et al. (1999b) and Guinotte et al. (2003), the corresponding *in situ* pH would be 8.02. The surface water *in situ* pH of most of the NoSoCS is between 8.05 and 8.07 (Fig. 8B). The rates of decrease in pH at the Hawaii Ocean Time-series station and the Bermuda Atlantic Time-series Station are around 0.002 y^{-1} (Bates and Peters, 2007; Dore et al., 2009). At SEATS in the northern SCS basin, a similar rate has been observed (D.D. Sheu, personal communication). At this rate of decrease in pH, *in situ* pH and Ω_{Ar} will probably drop to 8.02 and 3.0 respectively in 15–25 years. Similar results are found by considering the present average Ω_{Ar} in the surface NoSoCS and the rate of decrease in Ω_{Ar} at the time-series stations: the Hawaii Ocean Time-series station (Doney et al., 2009), the Bermuda Atlantic Time-series Station (Bates et al., 2012) and the SEATS station (unpublished data). This implies that, considering the effect of Ω_{Ar} alone, the existence of shallow water tropical coral reefs in the NoSoCS could become threatened within just a few decades. It should be noted that this is likely an over-simplified assessment as there are obviously other factors, such as temperature, that may also play an important role in the healthy growth of the corals reefs (Erez et al., 2011).

4. Conclusions and implications

The primary processes that influence the carbonate system in the NoSoCS are vertical mixing, biological uptake, and air–sea CO_2 exchange. A_T is mainly controlled by mixing between the lower salinity surface water with low A_T and the saline subsurface NPTW with high A_T. The composition of the surface water in the NoSoCS was significantly influenced by riverine input even during a low flow period when the samples were collected. In contrast, in the open northern SCS basin, A_T in the surface waters is controlled predominantly by precipitation and evaporation. C_T, on the other hand, is removed in the NoSoCS through biological uptake and CO_2 evasion, although the former is by far the more dominant process. Within the NoSoCS, the average removal rate of C_T by biological uptake is 9.5 mmol C m^{-2} d^{-1} and higher values (averaging 30.3 mmol C m^{-2} d^{-1}) are observed in the coastal upwelling area.

While the NoSoCS is super-saturated everywhere with respect to aragonite, the observed values of Ω_{Ar} in much of the NoSoCS fall within the range that has been suggested to be only "marginal" for the growth of the tropical shallow water corals which are found extensively in the NoSoCS. At the projected rates of decrease in pH and in the aragonite saturation state as a result of ocean acidification, Ω_{Ar} may drop to values that have been proposed to be "extremely marginal" for coral growth within a few decades and the existence of these tropical shallow water coral reefs in the NoSoCS potentially may then become threatened.

Acknowledgments

This work was supported by the National Science Council through Grants 98-2611-M-1-004-MY3 (to Wong). Guo was supported by a Postdoctoral Fellowship granted by the Academia Sinica. Preparation of the manuscript was supported by the National Natural Science Foundation of China through Grant 41206061 and the Fundamental Research Funds for the Central Universities (to Guo) and was completed while Wong was supported as a visiting professor at the Hong Kong University of Science and Technology. The cooperation of the crew and technical staff of R/V *Ocean Research I* is appreciated. We thank Dr. Jen-Hua Tai for providing the wind field data, and Drs. Wen-Chen Chou, Gwo-Ching Gong and Ms. Luo-Ping Chang for their assistance in the dissolved inorganic carbon and total alkalinity measurements. Comments from Dr. Eric Heinen De Carlo and two anonymous reviewers are constructive in improving the quality of the manuscript. Professor John Hodgkiss is thanked for his help in polishing the English.

References

Bates, N.R., Best, M.H.P., Neely, K., Garley, R., Dickson, A.G., Johnson, R.J., 2012. Detecting anthropogenic carbon dioxide uptake and ocean acidification in the North Atlantic Ocean. Biogeosciences 9 (7), 2509–2522.

Bates, N.R., Cai, W.-J., Mathis, J.T., 2011. The ocean carbon cycle in the western Arctic Ocean distributions and air–sea fluxes of carbon dioxide. Oceanography 24 (3), 186–201.

Bates, N.R., Peters, A.J., 2007. The contribution of atmospheric acid deposition to ocean acidification in the subtropical North Atlantic Ocean. Mar. Chem. 107 (4), 547–558.

Cai, W.-J., Dai, M.H., Wang, Y.C., 2006. Air–sea exchange of carbon dioxide in ocean margins: a province-based synthesis. Geophys. Res. Lett. 33 (12), http://dx.doi.org/10.1029/2006GL026219.

Cai, W.-J., Dai, M.H., Wang, Y.C., Zhai, W.D., Huang, T., Chen, S.T., Zhang, F., Chen, Z.Z., Wang, Z.H., 2004. The biogeochemistry of inorganic carbon and nutrients in the Pearl River estuary and the adjacent Northern South China Sea. Cont. Shelf Res. 24 (12), 1301–1319.

Cai, W.-J., Guo, X.H., Chen, C.-T.A., Dai, M.H., Zhang, L.J., Zhai, W.D., Lohrenz, S.E., Yin, K.D., Harrison, P.J., Wang, Y.C., 2008. A comparative overview of weathering intensity and HCO_3^- flux in the world's major rivers with emphasis on the Changjiang, Huanghe, Zhujiang (Pearl) and Mississippi Rivers. Cont. Shelf Res. 28 (12), 1538–1549.

Cai, W.-J., Hu, X.P., Huang, W.J., Jiang, L.Q., Wang, Y.C., Peng, T.H., Zhang, X., 2010. Alkalinity distribution in the western North Atlantic Ocean margins. J. Geophys. Res. 115 (C08), C08014. http://dx.doi.org/10.1029/2009JC005482.

Cai, W.-J., Hu, X.P., Huang, W.J., Murrell, M.C., Lehrter, J.C., Lohrenz, S.E., Chou, W.C., Zhai, W.D., Hollibaugh, J.T., Wang, Y.C., Zhao, P.S., Guo, X.H., Gundersen, K., Dai, M.H., Gong, G.C., 2011. Acidification of subsurface coastal waters enhanced by eutrophication. Nat. Geosci. 4 (11), 766–770.

Cao, Z.M., Dai, M.H., Zheng, N., Wang, D.L., Li, Q., Zhai, W.D., Meng, F.F., Gan, J.P., 2011. Dynamics of the carbonate system in a large continental shelf system under the influence of both a river plume and coastal upwelling. J. Geophys. Res. 116 (G02), G02010. http://dx.doi.org/10.1029/2010JG001596.

Chang, M.-H., Lien, R.-C., Yang, Y.J., Tang, T.Y., 2011. Nonlinear internal wave properties estimated with moored ADCP measurements. J. Atmos. Ocean. Technol. 28 (6), 802–815.

Chang, M.H., Lien, R.C., Tang, T.Y., D'Asaro, E.A., Yang, Y.J., 2006. Energy flux of nonlinear internal waves in northern South China Sea. Geophys. Res. Lett. 33, 3.

Chao, S.Y., Shaw, P.T., Wu, S.Y., 1996. Deep water ventilation in the South China Sea. Deep-Sea Res. I 43, 445–466.

Chen, C.-T.A., Borges, A.V., 2009. Reconciling opposing views on carbon cycling in the coastal ocean: continental shelves as sinks and near-shore ecosystems as sources of atmospheric CO_2. Deep-Sea Res. II 56 (8-10), 578–590.

Chen, C.T.A., Wang, S.L., 1999. Carbon, alkalinity and nutrient budgets on the East China Sea continental shelf. J. Geophys. Res. 104 (C9), 20675–20686.

Chen, C.T.A., Wang, S.L., Wang, B.J., Pai, S.C., 2001. Nutrient budgets for the South China Sea basin. Mar. Chem. 75 (4), 281–300.

Chen, W.F., Cai, P.H., Dai, M.H., Wei, J.F., 2008. $^{234}Th/^{238}U$ disequilibrium and particulate organic carbon export in the northern South China Sea. J. Oceanogr. 64 (3), 417–428.

Chen, Y.-L.L., 2005. Spatial and seasonal variations of nitrate-based new production and primary production in the South China Sea. Deep-Sea Res. I 52 (2), 319–340.

Chen, Y.-L.L., Chen, H.Y., 2006. Seasonal dynamics of primary and new production in the northern South China Sea: the significance of river discharge and nutrient advection. Deep-Sea Res. I 53 (6), 971–986.

Chou, W.C., Sheu, D.D., Lee, B.S., Tseng, C.M., Chen, C.T.A., Wang, S.L., Wong, G.T.F., 2007. Depth distributions of alkalinity, TCO_2 and delta ^{13}C-13 (TCO_2) at SEATS time-series site in the northern South China Sea. Deep-Sea Res. II 54 (14–15), 1469–1485.

Chow, C.H., Hu, J.H., Centurioni, L.R., Niiler, P.P., 2008. Mesoscale Dongsha cyclonic eddy in the northern South China Sea by drifter and satellite observations. J. Geophys. Res. 113 (C4), C04018. http://dx.doi.org/10.1029/2007JC004542.

Dai, M., Wang, L., Guo, X., Zhai, W., Li, Q., He, B., Kao, S.J., 2008a. Nitrification and inorganic nitrogen distribution in a large perturbed river/estuarine system: the Pearl River Estuary, China. Biogeosciences 5 (5), 1227–1244.

Dai, M.H., Zhai, W.D., Cai, W.-J., Callahan, J., Huang, B.Q., Shang, S.L., Huang, T., Li, X.L., Lu, Z.M., Chen, W.F., Chen, Z.Z., 2008b. Effects of an estuarine plume-associated bloom on the carbonate system in the lower reaches of the Pearl River estuary and the coastal zone of the northern South China Sea. Cont. Shelf Res. 28 (12), 1416–1423.

Dickson, A.G., 1990. Standard potential of the reaction AgCl (S)+1/2H_2(G)=Ag (S)+HCl (Aq), and the standard acidity constant of the ion HSO_4^- in synthetic seawater from 273.15 K to 318.15 K. J. Chem. Thermodyn. 22 (2), 113–127.

Dickson, A.G., Millero, F.J., 1987. A comparison of the equilibrium constants for the dissociation of carbonic acid in seawater media. Deep-Sea Res. A 34 (10), 1733–1743.

Dickson, A.G., Sabine, C.L., Christian, J.R., 2007. Guide to Best Practices for Ocean CO_2 Measurements, vol. 3. PICES Special Publication p. 191.

Doney, S.C., Balch, W.M., Fabry, V.J., Feely, R.A., 2009. Ocean acidification: a critical emerging problem for the ocean sciences. Oceanography 22 (4), 16–25.

Dore, J.E., Lukas, R., Sadler, D.W., Church, M., J., Karl, D.M., 2009. Physical and biogeochemical modulation of ocean acidification in the central North Pacific. Proc. Natl. Acad. Sci. USA 106 (30), 12235–12240.

Erez, J., Reynaud, S., Silverman, J., Schneider, K., Allemand, D., 2011. Coral calcification under ocean acidification and global change. In: Dubinsky, Z., Stambler, N. (Eds.). Coral Reefs: An Ecosystem in Transition, pp. 151–176.

Feely, R.A., Sabine, C.L., Lee, K., Millero, F.J., Lamb, M.F., Greeley, D., Bullister, J.L., Key, R.M., Peng, T.H., Kozyr, A., Ono, T., Wong, C.S., 2002. In situ calcium carbonate dissolution in the Pacific Ocean. Glob. Biogeochem. Cycles 16 (4), 1144. http://dx.doi.org/10.1029/2002GB001866.

Friis, K., Kortzinger, A., Wallace, D.W.R., 2003. The salinity normalization of marine inorganic carbon chemistry data. Geophys. Res. Lett. 30 (2), 1085. http://dx.doi.org/10.1029/2002GL015898.

Gan, J.P., Cheung, A., Guo, X.G., Li, L., 2009a. Intensified upwelling over a widened shelf in the northeastern South China Sea. J. Geophys. Res. 114 (C09), C09019. http://dx.doi.org/10.1029/2007JC004660.

Gan, J.P., Li, H., Curchitser, E.N., Haidvogel, D.B., 2006. Modeling South China sea circulation: response to seasonal forcing regimes. J. Geophys. Res. 111 (C6), C06034. http://dx.doi.org/10.1029/2005JC003298.

Gan, J.P., Li, L., Wang, D.X., Guo, X.G., 2009b. Interaction of a river plume with coastal upwelling in the northeastern South China Sea. Cont. Shelf Res. 29 (4), 728–740.

Gattuso, J.P., Frankignoulle, M., Bourge, I., Romaine, S., Buddemeier, R.W., 1998a. Effect of calcium carbonate saturation of seawater on coral calcification. Glob. Planet. Change 18 (1–2), 37–46.

Gattuso, J.P., Frankignoulle, M., Wollast, R., 1998b. Carbon and carbonate metabolism in coastal aquatic ecosystems. Annu. Rev. Ecol. Syst. 29, 405–434.

Green, R.E., Bianchi, T.S., Dagg, M.J., Walker, N.D., Breed, G.A., 2006. An organic carbon budget for the Mississippi River turbidity plume and plume contributions to air–sea CO_2 fluxes and bottom water hypoxia. Estuar. Coasts 29 (4), 579–597.

Gruber, N., Gloor, M., Fletcher, S.E.M., Doney, S.C., Dutkiewicz, S., Follows, M.J., Gerber, M., Jacobson, A.R., Joos, F., Lindsay, K., Menemenlis, D., Mouchet, A., Muller, S.A., Sarmiento, J.L., Takahashi, T., 2009. Oceanic sources, sinks, and transport of atmospheric CO_2. Glob. Biogeochem. Cycles 23, GB1005. http://dx.doi.org/10.1029/2008GB003349.

Guinotte, J.M., Buddemeier, R.W., Kleypas, J.A., 2003. Future coral reef habitat marginality: temporal and spatial effects of climate change in the Pacific basin. Coral Reefs 22 (4), 551–558.

Guo, L., Nie, B., Zhu, Y., Zhong, J., Zhou, D., Liang, Y., Zeng, C., 1994. Modern coral reefs in South China Sea. Oceanol. China Seas 2, 477–486.

Guo, X.H., Cai, W.-J., Zhai, W.D., Dai, M.H., Wang, Y.C., Chen, B.S., 2008. Seasonal variations in the inorganic carbon system in the Pearl River (Zhujiang) estuary. Cont. Shelf Res. 28 (12), 1424–1434.

Ho, D.T., Law, C.S., Smith, M.J., Schlosser, P., Harvey, M., Hill, P., 2006. Measurements of air-sea gas exchange at high wind speeds in the Southern Ocean: implications for global parameterizations. Geophys. Res. Lett. 33 (16), L16611. http://dx.doi.org/10.1029/2006GL026817.

Hsu, M.K., Liu, A.K., Liu, C., 2000. A study of internal waves in the China Seas and Yellow Sea using SAR. Cont. Shelf Res. 20 (4–5), 389–410.

Kleypas, J.A., Buddemeier, R.W., Archer, D., Gattuso, J.P., Langdon, C., Opdyke, B.N., 1999a. Geochemical consequences of increased atmospheric carbon dioxide on coral reefs. Science 284 (5411), 118–120.

Kleypas, J.A., McManus, J.W., Menez, L.A.B., 1999b. Environmental limits to coral reef development: where do we draw the line. Am. Zool. 39 (1), 146–159.

Langdon, C., Broecker, W.S., Hammond, D.E., Glenn, E., Fitzsimmons, K., Nelson, S.G., Peng, T.H., Hajdas, I., Bonani, G., 2003. Effect of elevated CO_2 on the community metabolism of an experimental coral reef. Glob. Biogeochem. Cycles 17 (1), 1011. http://dx.doi.org/10.1029/2002GB001941.

Laruelle, G.G., Durr, H.H., Slomp, C.P., Borges, A.V., 2010. Evaluation of sinks and sources of CO_2 in the global coastal ocean using a spatially-explicit typology of estuaries and continental shelves. Geophys. Res. Lett. 37 (L15607), L15607. http://dx.doi.org/10.1029/2010GL043691.

Leclercq, N., Gattuso, J.P., Jaubert, J., 2000. CO_2 partial pressure controls the calcification rate of a coral community. Glob. Change Biol. 6 (3), 329–334.

Li, X.F., Zhao, Z.X., Pichel, W.G., 2008. Internal solitary waves in the northwestern South China Sea inferred from satellite images. Geophys. Res. Lett. 35 (13), L13605. http://dx.doi.org/10.1029/2008GL034272.

Liu, Q., Dai, M., Chen, W., Huh, C.A., Wang, G., Li, Q., Charette, M.A., 2012. How significant is submarine groundwater discharge and its associated dissolved inorganic carbon in a river-dominated shelf system. Biogeosciences 9 (5), 1777–1795.

Liu, X.W., Patsavas, M.C., Byrne, R.H., 2011. Purification and characterization of meta-cresol purple for spectrophotometric seawater pH measurements. Environ. Sci. Technol. 45 (11), 4862–4868.

Mehrbach, C., Culberso, C.H., Hawley, J.E., Pytkowic, R.M., 1973. Measurement of apparent dissociation constants of carbonic acid in seawater at atmospheric pressure. Limnol. Oceanogr. 18 (6), 897–907.

Mucci, A., 1983. The solubility of calcite and aragonite in seawater at various salinities, temperatures, and one atmosphere total pressure. Am. J. Sci. 283 (7), 780–799.

Orr, J.C., Fabry, V.J., Aumont, O., Bopp, L., Doney, S.C., Feely, R.A., Gnanadesikan, A., Gruber, N., Ishida, A., Joos, F., Key, R.M., Lindsay, K., Maier-Reimer, E., Matear, R., Monfray, P., Mouchet, A., Najjar, R.G., Plattner, G.K., Rodgers, K.B., Sabine, C.L., Sarmiento, J.L., Schlitzer, R., Slater, R.D., Totterdell, I.J., Weirig, M.F., Yamanaka, Y., Yool, A., 2005. Anthropogenic ocean acidification over the twenty-first century and its impact on calcifying organisms. Nature 437 (7059), 681–686.

Pan, X., Wong, G.T.F., Shiah, F.K., Ho, T.Y., 2012. Enhancement of biological productivity by internal waves: observations in the summertime in the northern South China Sea. J. Oceanogr. 68 (3), 427–437.

Pierrot, D., Lewis, E., Wallace, D.W.R., 2006. MS Excel program developed for CO_2 system calculations. Carbon Dioxide Information Analysis Center, Oak Ridge National Laboratory, Oak Ridge, Tennessee. ORNL/CDIAC-105a, U.S. Department of Energy, 10.3334/CDIAC/otg.CO2SYS_XLS_CDIAC105a.

Qu, T.D., Girton, J.B., Whitehead, J.A., 2006. Deepwater overflow through Luzon Strait. J. Geophys. Res. 111 (C1), C01002. http://dx.doi.org/10.1029/2005JC003139.

Shamberger, K.E.F., Feely, R.A., Sabine, C.L., Atkinson, M.J., DeCarlo, E.H., Mackenzie, F.T., Drupp, P.S., Butterfield, D.A., 2011. Calcification and organic production on a Hawaiian coral reef. Mar. Chem. 127 (1-4), 64–75.

Shaw, P.T., Chao, S.Y., 1994. Surface circulation in the South China Sea. Deep-Sea Res. I 41 (11-12), 1663–1683.

Strickland, J.D.H., Parsons, T.R., 1972. A practical handbook of seawater analysis. Fisheries Research Board of Canada, Ottawa.

Sweeney, C., Gloor, E., Jacobson, A.R., Key, R.M., McKinley, G., Sarmiento, J.L., Wanninkhof, R., 2007. Constraining global air-sea gas exchange for CO_2 with

Please cite this article as: Guo, X., Wong, G.T.F., Carbonate chemistry in the Northern South China Sea Shelf-sea in June 2010. Deep-Sea Res. II (2015), http://dx.doi.org/10.1016/j.dsr2.2015.02.024

recent bomb C-14 measurements. Glob. Biogeochem. Cycles 21 (2), GB2015. http://dx.doi.org/10.1029/2006GB002784.

Takahashi, T., Sutherland, S.C., Sweeney, C., Poisson, A., Metzl, N., Tilbrook, B., Bates, N., Wanninkhof, R., Feely, R.A., Sabine, C., Olafsson, J., Nojiri, Y., 2002. Global sea–air CO_2 flux based on climatological surface ocean pCO_2, and seasonal biological and temperature effects. Deep. Sea Res. II 49 (9–10), 1601–1622.

Takahashi, T., Sutherland, S.C., Wanninkhof, R., Sweeney, C., Feely, R.A., Chipman, D. W., Hales, B., Friederich, G., Chavez, F., Sabine, C., Watson, A., Bakker, D.C.E., Schuster, U., Metzl, N., Yoshikawa-Inoue, H., Ishii, M., Midorikawa, T., Nojiri, Y., Kortzinger, A., Steinhoff, T., Hoppema, M., Olafsson, J., Arnarson, T.S., Tilbrook, B., Johannessen, T., Olsen, A., Bellerby, R., Wong, C.S., Delille, B., Bates, N.R., de Baar, H.J.W., 2009. Climatological mean and decadal change in surface ocean pCO_2, and net sea–air CO_2 flux over the global oceans. Deep-Sea Res. II 56 (8-10), 554–577.

Tan, S.C., Shi, G.Y., 2009. Spatiotemporal variability of satellite-derived primary production in the South China Sea, 1998-2006. J. Geophys. Res. 114 (G03), G03015. http://dx.doi.org/10.1029/2008JG000854.

Thomas, H., Bozec, Y., Elkalay, K., de Baar, H.J.W., 2004. Enhanced open ocean storage of CO_2 from shelf sea pumping. Science 304 (5673), 1005–1008.

Tribollet, A., Atkinson, M.J., Langdon, C., 2006. Effects of elevated pCO_2 on epilithic and endolithic metabolism of reef carbonates. Glob. Change Biol. 12 (11), 2200–2208.

Tseng, C.M., Wong, G.T.F., Chou, W.C., Lee, B.S., Sheu, D.D., Liu, K.K., 2007. Temporal variations in the carbonate system in the upper layer at the SEATS station. Deep-Sea Res. II 54, 1448–1468.

Tseng, C.M., Wong, G.T.F., Lin, I.I., Wu, C.R., Liu, K.K., 2005. A unique seasonal pattern in phytoplankton biomass in low-latitude waters in the South China Sea. Geophys. Res. Lett. 32 (8), L08608. http://dx.doi.org/10.1029/2004GL022111.

Wang, Y.H., Dai, C.F., Chen, Y.Y., 2007. Physical and ecological processes of internal waves on an isolated reef ecosystem in the South China Sea. Geophys. Res. Lett. 34, L18609. http://dx.doi.org/10.1029/2007GL030658.

Wang, Z.H.A., Wanninkhof, R., Cai, W.-J., Byrne, R.H., Hu, X.P., Peng, T.H., Huang, W.J., 2013. The marine inorganic carbon system along the Gulf of Mexico and Atlantic coasts of the United States: Insights from a transregional coastal carbon study. Limnol. Oceanogr. 58 (1), 325–342.

Wanninkhof, R., 1992. Relationship between wind speed and gas exchange over the ocean. J. Geophys. Res. 97 (C05), 7373–7382.

Weiss, R.F., 1974. Carbon dioxide in water and seawater: the solubility of a non-ideal gas. Mar. Chem. 2, 203–215.

Weiss, R.F., Price, B.A., 1980. Nitrous oxide solubility in water and seawater. Mar. Chem. 8 (4), 347–359.

Wong, G.T.F., Ku, T.-L., Liu, H., Mulholland, M., this issue-a. The Oceanography of the Northern South China Sea Shelf-sea (NoSoCS) and Adjacent Waters: An Overview.

Wong, G.T.F., Pan, X., Li, K.-Y., Shiah, F.K., Ho, T.-Y. and Guo, X., this issue-b. Hydrography and nutrient dynamics in the Northern South China Sea Shelf-sea (NoSoCS) [doi: http://dx.doi.org/10.1016/j.dsr2.2015.02.023].

Wong, G.T.F., Tseng, C.M., Wen, L.S., Chung, S.W., 2007. Nutrient dynamics and N-anomaly at the SEATS station. Deep-Sea Res. II 54 (14–15), 1528–1545.

Wong, T.F.G., 1979. Alkalinity and pH in the Southern Chesapeake Bay and the James River estuary. Limnol. Oceanogr. 24, 970–977.

Wong, T.F.G., 1988. Alkalinity in the South-eastern United States continental Shelf waters. Estuar. Coast. Shelf Sci. 27, 567–579.

Xue, H.J., Chai, F., Pettigrew, N., Xu, D.Y., Shi, M., Xu, J.P., 2004. Kuroshio intrusion and the circulation in the South China Sea. J. Geophys. Res. 109 (C2), C02017. http://dx.doi.org/10.1029/2002JC001724.

Zhai, W.D., Dai, M.H., 2009. On the seasonal variation of air-sea CO_2 fluxes in the outer Changjiang (Yangtze River) Estuary, East China Sea. Mar. Chem. 117 (1-4), 2–10.

Zhao, H., 1990. Evolution of the Pearl River Estuary. Ocean Press, Beijing p. 357, in Chinese.

Please cite this article as: Guo, X., Wong, G.T.F., Carbonate chemistry in the Northern South China Sea Shelf-sea in June 2010. Deep-Sea Res. II (2015), http://dx.doi.org/10.1016/j.dsr2.2015.02.024